Journal of Chemical Health Risks

www.jchr.org

JCHR (2025) 15(5), 158-167 | ISSN:2251-6727

Design of a Biphasic Calcium Phosphate Scaffold with Embedded Hyaluronic Acid-Chitosan Microspheres Infused Hydrogel

Shubhangee Tomar[1*], Krishna Vaghela[2], Varsha Patel[3], Payal S Makwana[4], Het P Solanki[1], Divyang Dave[1]

[1]*Department of Pharmaceutics, KB Institute of Pharmaceutical Education and Research, KSV, Gandhinagar, Gujarat, India*

[2]*Department of Pharmacology, Saraswati Institute of Pharmaceutical Sciences Dhanap and National Forensic Sciences University, Gandhinagar, Gujarat, India*

[3]*Department of Pharmaceutics, Merchant Pharmacy college, Mehsana, Gujarat, India,*

[4]*Assistant Professor, Department of Pharmacology and Pharmacy Practice, KB Institute of Pharmaceutical Education and Research, KSV, Gandhinagar, Gujarat, India*

(Received: 16 July 2025 Revised: 20 August 2025 Accepted: 02 September 2025)

KEYWORDS
Bone Tissue Engineering, Scaffold, Biomaterials, Microspheres, Biphasic Calcium Phosphate, Chitosan

ABSTRACT:

Introduction: Bone-related issues, including osteomyelitis, injuries, and tumours, cause considerable harm to skeletal structures, making replacement procedures essential to restore their normal shape and function. This study aimed to create an innovative biphasic calcium phosphate (BCP) scaffold infused with a hydrogel containing hyaluronic acid-chitosan microspheres to enhance bone regeneration. Achieving this requires a careful balance between the scaffold's release rate and the deposition rate of cells on the new native extracellular matrix. Microspheres can help achieve this by regulating the scaffold's release rate and providing ample time for new cells to settle on the extracellular matrix.

Objectives: To create Biphasic calcium phosphate scaffold with hyaluronic acid-chitosan microspheres infused hydrogel for improved bone regeneration.

Methods: BCP scaffold was prepared by sponge replica method. Prepared microspheres were checked for size, morphology and encapsulation efficiency. To check osteogenic differentiation and proliferation of microspheres incorporated BCP Scaffold swelling and degradation rates, ALP staining, cell viability (MTT Assay) and immunocytochemical analysis was conducted.

Results: The in vitro cytocompatibility study revealed that BMSCs adhered to and proliferated on the scaffolds, with cell viability confirmed by the MTT Assay and ALP staining. Additionally, immunocytochemical analysis showed satisfactory osteogenic differentiation on day 7 and 14. In every aspect of evaluation HyA-Ch-Ms hydrogel coated BCP scaffold show better cell regeneration as compared to plane BCP scaffold.

Conclusions: The tissue engineering method is regarded as an advanced technique for repairing bone defects because it utilizes the patient's own tissue for the healing process. In this study, we have successfully created an innovative combination of biomaterials that demonstrates promising outcomes and can be applied to bone regeneration.

1. Introduction

In recent times, there has been an increasing need for bone regeneration due to various bone-related conditions such as infections, tumours, and bone loss. The process of bone tissue engineering is intricate and involves several stages, beginning with the movement and gathering of osteoprogenitor cells. This is followed by their growth, specialization, and the formation of the matrix, along with the subsequent remodelling of the bone [1]. The process of bone healing is both dynamic and stable, continuing throughout a person's life. While certain individual factors can heighten the risk of healing complications, the exact causal connections remain not

Journal of Chemical Health Risks
www.jchr.org
JCHR (2025) 15(5), 158-167 | ISSN:2251-6727

fully understood [2]. Despite significant advancements in bone regenerative medicine over the years, existing treatments like bone grafts continue to face numerous challenges. In this scenario, tissue engineering has emerged as a promising alternative to current methods for bone regeneration or replacement [3]. In the design process of engineered bone substitutes, it is customary to include material requirements, but it is equally important to integrate clinical requirements to create a device that is relevant in a clinical setting [4]. Advancements in bone tissue engineering have facilitated the creation of functional substitutes for bone regeneration. This is accomplished by developing bone tissue scaffolds that promote osteoconduction and integration, offer mechanical support, and either merge with the bone structure or break down and are eliminated by the body [5]. Osseous tissue consists of an organic phase of mainly collagen fibres, which impart strength, flexibility, and resistance to torsional force, and an inorganic phase of mainly hydroxyapatite, which provides resistance to compression [6]. For bone applications, materials should ideally possess osteoinductive and osteoconductive properties, as well as the ability to integrate with bone tissue [7]. Bone tissue consists of both inorganic and organic components. The inorganic portion is primarily made up of hydroxyapatite, along with citrate, carbonate, and various ions.

The organic part of bone includes type I collagen and non-collagenous proteins such as osteocalcin, osteonectin, bone scleroproteins, and a range of proteoglycans. These elements play a crucial role in the maturation of the matrix and may influence the functional activities of bone cells [8]. Materials sourced from nature for BTE encompass polymers like silk and chitosan, as well as purified ECM-based molecules such as collagen, elastin, and GAGs [9]. Biphasic calcium phosphate (BCP) ceramics, which consist of hydroxyapatite (HA) and beta-tricalcium phosphate (beta-TCP), demonstrated remarkable osteoinductivity, osteoconductivity, bioactivity, and biodegradability [10]. Hyaluronic acid (HyA) is a key component of the extracellular matrix and is found throughout the human body. Due to its distinct physical and chemical characteristics and its wide range of physiological roles, hyaluronic acid is extensively utilized in tissue engineering and regenerative medicine [11]. Chitosan is an attractive polymer for tissue engineering due to its nontoxic nature, compatibility with biological systems, and ability to break down naturally. Additionally, chitosan shares a structural resemblance with glycosaminoglycans, which are the primary constituents of the extracellular matrix (ECM) [12]. Chitosan, a natural biopolymer, holds great potential as a biomaterial for engineering bone tissue [13]. Recent studies have demonstrated that the structure of porous scaffolds employed in bone tissue engineering and replacement plays a crucial role in affecting cellular behaviour and the speed of bone tissue regeneration [14].

The field of medicine is experiencing a major shift, transitioning from the use of synthetic implants and tissue grafts to a focus on tissue engineering. This innovative method employs degradable porous material scaffolds in conjunction with biological cells or molecules to facilitate tissue regeneration [15]. Tissue engineering is a field within biomedical engineering that concentrates on the repair and regeneration of organs or their tissues [16]. Biomaterial scaffolds function as a framework for cells, guiding their growth by ensuring they receive sufficient nutrients, oxygen, metabolic byproducts, and suitable growth factors to promote their differentiation and performance [17]. The three essential criteria for BTE scaffolds are their ability to induce bone formation, support bone growth, and be compatible with biological tissues [18].

In the realm of tissue engineering, microspheres are widely utilized as drug delivery systems due to their exceptional ability to control the release of drugs [19]. Smart hydrogel microspheres are small spherical particles made from cross-linked hydrophilic polymers, known for their outstanding biocompatibility, ease of injection, capacity to load drugs, ability to degrade, and responsiveness to stimuli [20]. Bone-mimicking porous hydrogels effectively enhance the regeneration of vascularized bone in an ectopic subcutaneous setting [21]. In this study, we incorporated Chitosan-Hyaluronic acid microspheres with controlled release properties into porous BCP scaffolds to achieve an optimal balance between the release of biomaterial content and the adherence of cells to the newly formed extracellular matrix. This combination allows cells ample time to develop, proliferate, and migrate within the newly created extracellular matrix.

2. Methods

Materials: Chitosan, with a degree of deacetylation exceeding 88%, was sourced from Bangalore Fine Chemicals. BCP was acquired from Nano Research Lab in Jharkhand. The sodium salt of hyaluronic acid came from R P Chemicals in Maharashtra. PVB was received

Journal of Chemical Health Risks
www.jchr.org
JCHR (2025) 15(5), 158-167 | ISSN:2251-6727

as a complimentary sample from Siva Chemical Industries, also in Maharashtra. Gelatin type A was obtained from Chemdyes Chemicals.

Formulation of BCP Scaffold: The Sponge Replica Method was used to pre- pare the BCP scaffold [22]. The BCP slurry was created by combining 10% BCP with 5% Poly Vinyl Butyral. This mixture was then used to soak the polyurethane sponge, which was an HD sponge with a density of 60 ppi. The scaffolds were subjected to a sintering process in a microwave oven at 1200°C for 10 minutes, with a heating rate of 100°C per minute. To remove impurities from the sponge scaffolds, they underwent ultrasonic cleaning in distilled water, followed by a drying process.

Preparation of Chitosan-Hyaluronic acid (Ch-HyA) microspheres: The microspheres were produced using the emulsion-ionic cross-linking technique, with TPP serving as the cross-linking agent [23]. To prepare the solution, 500 mg of chitosan was dissolved in 20 mL of 2% (v/v) aqueous acetic acid and stirred until it became transparent. Simultaneously, 100 mg of hyaluronic acid was dissolved in 5 mL of 2% (v/v) acetic acid and then combined with the chitosan solution. This mixture was then stirred for two hours in 200 mL of liquid paraffin containing 2% (w/v) span-80. Subsequently, 50 mL of 5% (w/v) TPP was introduced to the emulsion, which was stirred for an additional four hours at room temperature. The final emulsion was thoroughly washed multiple times using excess petroleum ether, isopropyl alcohol, and distilled water. After lyophilization, microspheres were obtained.

Combining BCP Scaffold with Ch-HyA Microspheres Hydrogel: At a temperature of 30°C, a 10% by weight solution of gelatin with a Bloom strength of 300 was prepared using deionized water [24]. The Gelatin solution was combined with sufficient amounts of HyA (0.5% by weight) to create a slurry with a volume ratio of 15:85 (HyA: Gel). This gelatin slurry was then blended with 250 mg of Ch-HyA microspheres. Once the microspheres were thoroughly dispersed using magnetic stirring, the mixture was poured onto the BCP scaffold. The mixture was then refrigerated at -20°C overnight. Ultimately, BCP-Ch-HyA microspheres loaded scaffolds were produced following lyophilization.

Morphology: The morphology of the BCP Scaffold, Ch-HyA Microspheres, and their final combination was examined using an inverted light microscope and a scanning electron microscope.

porosity and pore size distribution: A mercury porosimeter is utilized to examine the porosity and pore size distribution of scaffolds. The scaffolds are positioned in a penetrometer and subjected to mercury infiltration as the pressure is gradually increased.

Chemical analysis: Fourier transform infrared (FT-IR) spectroscopy is employed to identify the chemical properties of all scaffolds using the transmittance mode within the mid-infrared range of 4000–500 cm-1. For FTIR analysis, the samples were cut into 2 × 2 cm^2 squares.

Encapsulated Efficiency (EE): 5ml of a 2% aqueous acetic acid solution were employed to dissolve a certain amount of Ch-HyA microspheres hydrogel, and any leftover residue was removed through filtration. The HyA levels in the collected sample were then measured using HPLC. supernatants were determined. Encapsulated efficiency (EE) was calculated as follows: percentage EE = actual HyA amount × 100/ theoretical HyA amount

In vitro bioactivity: Simulated Body Fluid was prepared by following Kokubo and Takadama, 2006) [25]. Scaffolds were sectioned into 1 × 1 cm2 pieces and placed in polyethylene tubes filled with 30 mL of freshly prepared Simulated Body Fluid (SBF) to form samples. Samples were extracted after immersion periods of 2, 4, 7, and 14 days. For each time point, five samples from each scaffold were evaluated. All samples were maintained in a shaking incubator at 37°C and 90 rpm. The SBF was replaced every 48 hours. After each designated immersion period, the samples were removed, thoroughly rinsed with distilled water, blotted with filter paper, and dried in the incubator at 37°C until they reached a constant weight. Subsequently, the samples were coated with gold and analysed using SEM [26].

Cell Viability using MTT assay: The MTT assay is utilized to assess cell viability. Surfaces of both the test and control materials are seeded with 104 cells/mL (BMSCs) in media. To evaluate cell viability (OD) on the scaffold at 1, 4, and 7 days, 100 mL of MTT solution (5 mg/mL in PBS) is introduced into each well of a 24 well tissue culture plate. An ELISA reader, calibrated to 595

Journal of Chemical Health Risks
www.jchr.org
JCHR (2025) 15(5), 158-167 | ISSN:2251-6727

nm, will be employed to determine the optical density (OD) values of the solution[27].

Evaluation of scaffold swelling and degradation rates: To evaluate the swelling rates of different scaffolds, the initial weights of the samples are measured before they are immersed in SBF. After intervals of two, seven, and fourteen days, the samples are extracted from the SBF, rinsed with distilled water, and dried using filter paper to eliminate any residual moisture. The samples are then weighed, and the swelling ratio (S) is calculated using the formula: percentage S = (WS - W0) / W0 * 100, where W0 represents the sample's weight (in grams) prior to immersion in SBF, and WS denotes the weight of the swollen sample (in grams). Once removed from SBF, the samples are rinsed with distilled water, blotted with filter paper, and dried in an incubator until they reach a stable mass for the degradation rate assessment. After complete drying, the sample weights are recorded. The weight loss (WL) is determined using the formula: percentage WL = (W0 - WD) / W0 * 100, where W0 is the weight (in grams) of the sample before immersion, and WD is the weight (in grams) of the sample after being removed from the SBF and fully dried[28].

Cell Proliferation Study: To determine whether the hydrogel loading influenced the adhesion and proliferation of BMSCs on the scaffolds, BMSCs were grown on BCP scaffolds loaded with Ch-HyA microspheres. The adhesion and proliferation of BMSCs on these scaffolds were evaluated using a confocal microscope after 1, 4, and 7 days of incubation[29] [30]. F-actin was distinctly observed in the membranes of BMSCs. Immunocytochemical analysis was conducted on days 14 and 21 [31] and ALP staining (Alkaline Phosphate Staining Kit) [32] are used to assess the osteogenic differentiation of BMSCs.

Osteogenic differentiation: The osteogenic differentiation of BMSCs can be assessed using an ALP (Alkaline Phosphate) Staining Kit and immunocytochemical analysis on days 14 and 21 [33]. To conduct an immunocytochemical examination of osteopontin (OPN) and osteocalcin (OCN), which are specific to bone tissue proteins. The scaffolds are treated overnight at 4ºC with mouse anti-OPN and anti-OCN antibodies, both at a dilution of 1:200. Subsequently, they are exposed to a 91:1000 dilution of an anti-mouse secondary antibody. A confocal fluorescent microscope, along with its associated Viewer software, is employed to examine the images. For immunostaining, fluorescein isothiocyanate (FITC)-conjugated phalloidin at a concentration of 25 mg/mL is utilized, while 4', 6'-diamidino-2-phenylindole (DAPI) serves as a nuclear counterstain[34].

3. Results

Morphology, porosity and pore size distribution: The shapes of microspheres, BCP scaffolds, and BCP scaffolds loaded with microspheres were examined using an optical microscope and SEM, as depicted in Fig 1. The Ch microspheres exhibited a relatively rough and sharp surface (fig. 1c), with sizes that were uniformly distributed. The average diameter of the Ch microspheres was 48.52 µm. The findings indicated an entrapment efficiency of 83.2 ± 2% which is crucial for controlled delivery. Cross-linking was employed to securely entrap HyA within the Ch microspheres. The pore size is a key factor in the effectiveness of cell seeding into the scaffold. While excessively large pores reduce cell attachment due to a smaller area for cell colonization, very small pores impede the cells' ability to infiltrate the scaffold. The BCP scaffold was created using freeze-drying techniques and a sponge replica. Most of the open, interconnected pores, which were ideal for tissue formation and cell penetration, ranged from 150 to 280 µm (fig. 1a and b). The porosity only slightly decreased from 85.81±0.61 to 83.93±0.32% following the incorporation of chitosan microspheres.

Morphological Characterization

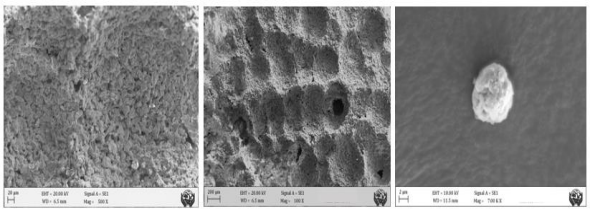

Fig. 1 a) and b) represent scanning electron microscopy images of BCP scaffold, c) shows SEM image for Ch-HyA Microsphere

Chemical analysis: FTIR serves as a powerful method for determining the organic composition of different compounds. Figure 2 presents the FTIR outcomes for BCP, Chitosan, Hyaluronic acid, and a BCP scaffold integrated with Ch-HyA microspheres, confirming the success of all interaction processes. Fingerprint Region 419.25 cm^{-1}, 1033.87 cm^{-1}.

Journal of Chemical Health Risks
www.jchr.org
JCHR (2025) 15(5), 158-167 | ISSN:2251-6727

Chemical Analysis

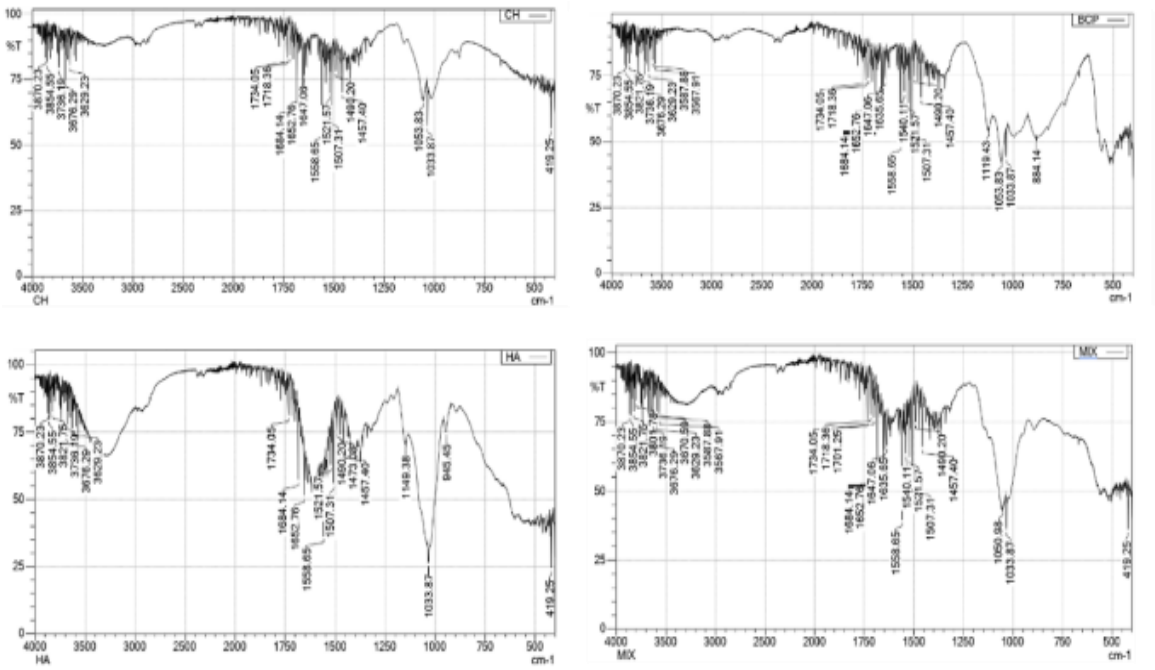

Figure 2 represents FTIR results for Chitosan, BCP, Hyaluronic Acid and the Ch-HyA microspheres loaded BCP Scaffold

1050.98 cm^{-1} indicate unique structural features of Hyaluronic acid. Functional Group Region Peaks at 1507.31 cm^{-1}, 1521.57 cm^{-1}, 1540.11 cm^{-1}suggest aromatic or C=C stretching. 1652.76 cm^{-1}, 1684.14 cm^{-1} may indicate C=O stretching (carbonyl). 3567.91 cm^{-1}, 3587.88 cm^{-1}, 3629.23 cm^{-1}, 3670.59 cm^{-1} suggest O-H or N-H stretching (hydroxyl or amine groups). The presence of peaks in the region of 1700-1750 cm^{-1} suggests carbonyl groups (C = O), while peaks beyond 3500 cm^{-1} indicate hydroxyl (-OH) or amine (-NH) groups, confirm the presence of BCP and chitosan

Encapsulated Efficiency (EE): The microspheres' sizes were evenly dis- tributed. CMs had an average diameter of 48.52 µm. The results showed an entrapment efficiency of 83.2 ± 2%.

In vitro bioactivity and Cell Viability:

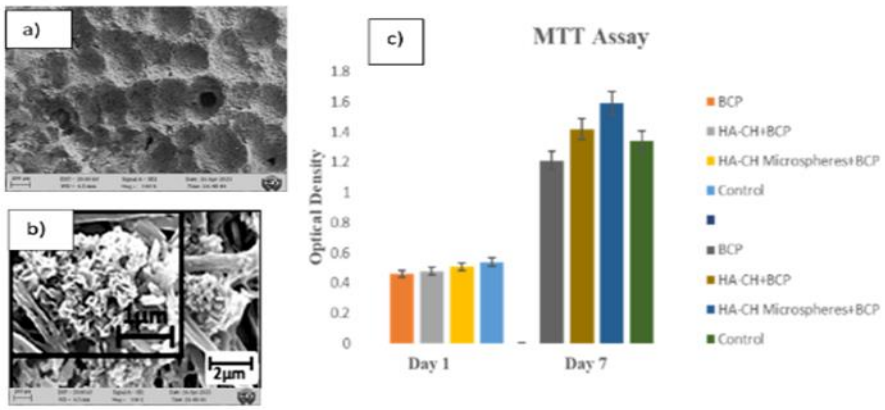

Fig. 3 In vitro bioactivity shown before and after immersing the scaffold in SBF for 14 days (a, b). c) represents MTT Assay results of BCP, Chitosan, Hyaluronic acid and Ch-HyA microsphere loaded BCP scaffold were compared for day 1 and day 7

Journal of Chemical Health Risks
www.jchr.org
JCHR (2025) 15(5), 158-167 | ISSN:2251-6727

In Vitro Bioactivity and Cell Viability: When the BCP scaffold was submerged in SBF, changes in surface morphology were observed in the SEM images, indicating a layer that gradually formed over time. By the 14th day, this layer had extended across almost the entire scaffold surface. A distorted globular layer appeared on the Ch-HyA-Ms-BCP scaffold, resulting in favorable bioactivity outcomes. After a week of incubation, the MTT assay was conducted to evaluate the proliferation of BMSCs on the scaffolds, as shown in Fig. 3c. From the first to the seventh day of culture, BMSCs consistently proliferated on all scaffolds, with the hydrogel containing Ch-HyA-Ms and BCP scaffolds exhibiting the highest Optical Density.

Evaluation of scaffold swelling and degradation rates: A key indicator for evaluating the degradation performance f scaffolds is the rate of weight loss. This metric reflects the WL of BCP scaffolds both with and without Ch-HyA-Ms. As the degradation period extended, the mass of the BCP scaffolds diminished. During the initial week, the pure BCP scaffold exhibited a slower WL compared to the scaffold containing microspheres. The rate increased in the second week, slowed again after three weeks, and then continued to release gradually over the following six weeks. (figure 4). The BCP scaffolds with and without microspheres had respective WL rates of 6.72% and 8.91% at week 6.

Swelling and Degradation Properties

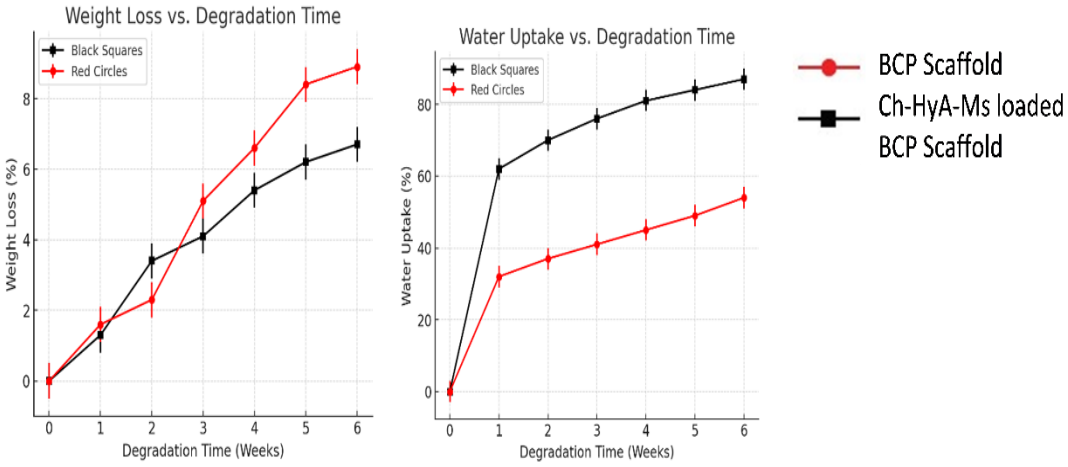

Fig. 4 Figure 4 represents Weight loss and water absorption results upto 6 weeks to evaluate swelling and degradation properties

Thus, the use of microspheres was successful in achieving the objective of a slower release of scaffold content.

Another vital aspect in designing a suitable scaffold for bone regeneration is its WA properties. This refers to the WA of BCP scaffolds both with and without CMs. Initially, at week one, the WA of the BCP scaffold containing microspheres was 62.36%, and it progressively rose to 87.72% by week six. Conversely, the WA of the BCP scaffold decreased over time, dropping to 54.23% by the sixth week. The scaffold's WA was crucial for the initial integration of the material-bone construct.

Cell Proliferation and Osteogenic Differentiation Study: Following a four-day incubation period, the attachment and growth of BMSCs on the scaffolds were evaluated using a confocal microscope. Figure 5 illustrates the MSCs' structures. On the first day of culture, F-actin was visible in the BMSC membranes, signifying cell health. By the fourth day of culture, the confocal images showed that more cells had adhered directly to the porous surfaces compared to the first day.

Journal of Chemical Health Risks
www.jchr.org
JCHR (2025) 15(5), 158-167 | ISSN:2251-6727

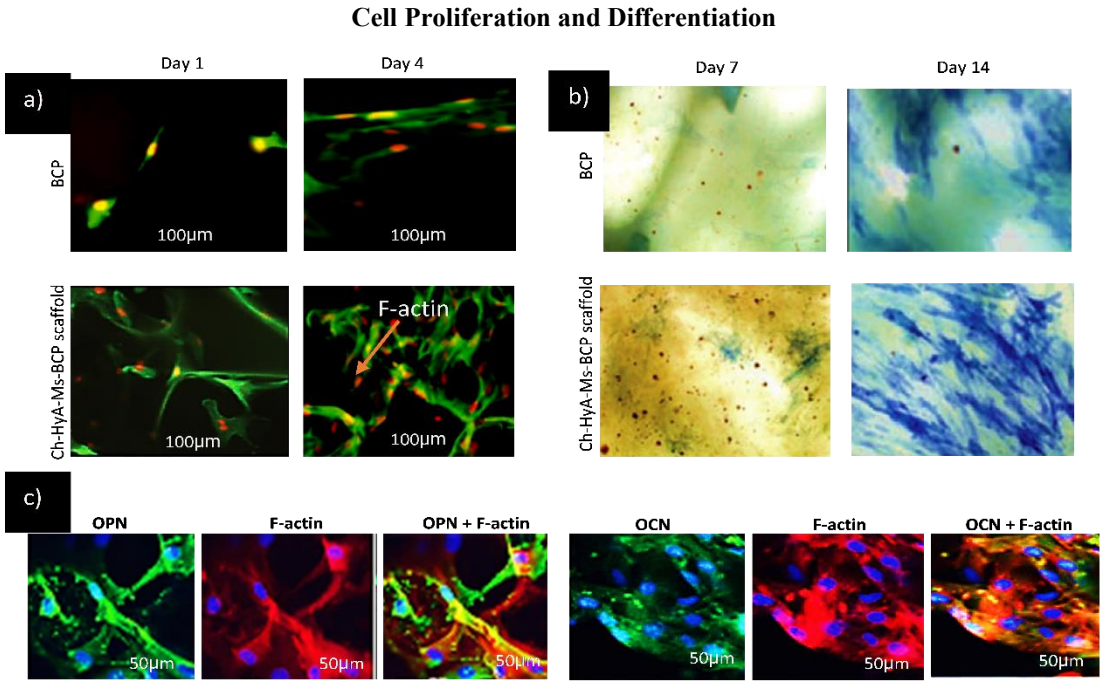

Fig. 5 Figure 5 a) illustrates the morphologies of BMSCs as captured by a confocal microscope on Days 1 and 4 for the BCP Scaffold Ch-HyA-Ms-BCP Scaffold. b) displays optical microscope images depicting ALP staining, which indicates the differentiation of osteoblasts by BMSCs on Days 7 and 14 on both BCP and Ch-HyA-Ms-BCP scaffolds. c) shows immunostaining of cells, allowing for the visualization of protein localization through confocal images with osteopontin (OPN) and osteocalcin (OCN).

Following a fortnight of osteogenic culture, BMSCs exhibited positive ALP (blue) within the monolayer. Optical microscope images display ALP staining for osteoblast differentiation by BMSCs on days 7 and 14 on both BCP and Ch-HyA-Ms-BCP scaffolds. The ALP staining signified early-stage bone cell differentiation. Ch-HyA-Ms-BCP scaffolds demonstrated greater ALP activity compared to plain BCP scaffolds. Confocal images were used to visualize protein localization after cells were immunostained with osteopontin (OPN) and osteocalcin (OCN). As bone-specific proteins and indicators of relatively late-stage osteogenic differentiation, primary antibodies against OPN and OCN were employed. On days 7 and 14, both OPN and OCN exhibited more pronounced growth on the Ch-HyA-Ms-BCP scaffold than on the plain BCP scaffold.

4. Discussion

The research focuses on developing scaffolds that mimic natural bone structure for optimal clinical application. The scaffolds incorporate hyaluronic acid-chitosan microspheres within a biphasic calcium phosphate (BCP) structure, successfully integrating and distributing them without compromising scaffold integrity. The inclusion of up to 30% chitosan microspheres maintained high porosity due to the interconnected three-dimensional pore structure. The scaffolds demonstrated compressive strength comparable to cancellous bone, attributed to the network formed by hyaluronic acid, chitosan, and BCP. The composition can be adjusted to modify mechanical strength for specific regenerative purposes. Chitosan was chosen for microsphere creation due to its biocompatibility, biodegradability, low toxicity, and cost-effectiveness. The degradation process of the scaffold plays a crucial role in bone regeneration. It occurs in four phases: polymer swelling, bond breaking, diffusion of degradation products, and disappearance of scaffold fragments. This process facilitates cell development, attachment, and growth using microspheres.

In vitro studies showed uniform distribution of bone marrow stromal cells (BMSCs) across the scaffolds, with cells proliferating within the hydrogel and attaching to the microporous structure. Confocal microscopy revealed cell colonization on the surface and within the

Journal of Chemical Health Risks
www.jchr.org
JCHR (2025) 15(5), 158-167 | ISSN:2251-6727

scaffold, with normal, healthy cell morphology observed. The combination of materials in these scaffolds enhances both osteoconductivity and osteoinductivity, crucial for effective bone repair. The use of microspheres allows for controlled release of bioactive factors, potentially improving the regeneration process over time. Future research should focus on refining scaffold composition and production techniques to enhance efficacy. In vivo studies are necessary to assess long-term functionality and integration in bone defects. Overall, the development of BCP scaffolds with hyaluronic acid and chitosan microspheres shows significant potential for advancing bone regeneration techniques.

5. Conclusion

The innovative hybrid scaffold combining BCP with HA-CS-MS demonstrates significant potential for bone tissue engineering applications. This novel approach, which integrates chitosan hyaluronic acid microspheres into the BCP scaffold, exhibits enhanced osteogenic potential, biocompatibility, and mechanical properties. In vitro and in vivo studies provide compelling evidence of increased cellular proliferation and accelerated bone regeneration. The scaffold's improved bioactivity and ability to bond with native bone tissue further support its efficacy. Immunostaining analysis corroborates these findings, revealing a strong correlation between the scaffold and tissue regeneration. While the Ch-HyA-Ms-BCP scaffolds show promise as an excellent platform for bone regeneration, further preclinical studies are necessary to fully evaluate their potential for patient recovery. The adaptability of this scaffold system allows for customization of hydrogel or sponge components to suit various in vivo osteogenesis applications. To advance towards clinical use, future research should focus on long-term in vivo studies and optimization of scaffold properties.

Abbreviations

Ch- Chitosan
HyA- Hyaluronic acid
Ms- Microsphere
BCP- Biphasic Calcium Phosphate
ALP Staining- Alkaline phosphatase staining
OPN- Osteopontin
OCN- Osteocalcin
WA study- water absorption study
WL study- weight loss study
BMSCs- Bone marrow mesenchymal stromata cells
MTT- (3-[4, 5-dimethylthiazol-2-yl]-2, 5-diphenyltetrazolium bromide)

Acknowledgement

Authors acknowledge support provided by Biochemistry department MSU Baroda, National Centre for Cell Science (NCCS), Gujarat Biotechnology Research Centre (GBRC) and GEER Foundation.

Author Contributions

ST conceived and designed the research work, Collected the data, contributed data or analysis tools, Performed the method, drafted the manuscript, DD guided design of work and helped in understanding the results, KV and PSM performed cell line study and cell cytotoxicity study, carried out analytical data collection and interpretation. VP carried out materials procurement and participated in morphological characterization and helped in drafting manuscript, HP conducted thorough Literature analysis and performed Preformulation studies. All authors read and approved the final manuscript.

Competing Interest

The Authors declare no potential conflicts of interest with respect to the research, authorship, and/or publication of this article

Ethics Statement

This study does not involve any living invertebrate, human participants or patients' data and does not require ethical approvals

Availability of Supporting data

The datasets used and/or analysed during the current study available from the corresponding author on reasonable request

Funding

This study was not financially supported by any organization

References

1. Gong T, Xie J, Liao J, Zhang T, Lin S, Lin Y. Nanomaterials and bone regeneration. Bone Research. 2015 Mar;3(1):15029.
2. Duda GN, Geissler S, Checa S, Tsitsilonis S, Petersen A, Schmidt-Bleek K. The decisive early phase of bone regeneration. Nature

Journal of Chemical Health Risks

www.jchr.org

JCHR (2025) 15(5), 158-167 | ISSN:2251-6727

Reviews Rheumatology. 2023 Mar;19(2):78–95.
3. Salgado AJ, Coutinho OP, Reis RL. Bone Tissue Engineering: State of the Art and Future Trends. Macromolecular Bioscience. 2004 Mar;4(8):743–65.
4. Burg KJL, Porter S, Kellam JF. Biomaterial developments for bone tissue engineering. Biomaterials. 2000 Mar;21(23):2347–59.
5. Kačarević ŽP, Rider P, Alkildani S, Retnasingh S, Pejakić M, Schnettler R, et al. An introduction to bone tissue engineering. The International Journal of Artificial Organs. 2020 Mar;43(2):69–86.
6. Le B, Nurcombe V, Cool S, Blitterswijk C van, Boer J de, LaPointe V. The Components of Bone and What They Can Teach Us about Regeneration. Materials. 2017 Mar;11(1):14.
7. Stevens MM. Biomaterials for bone tissue engineering. Materials Today. 2008 Mar;11(5):18–25.
8. Iaquinta MR, Mazzoni E, Manfrini M, D'Agostino A, Trevisiol L, Nocini R, et al. Innovative Biomaterials for Bone Regrowth. International Journal of Molecular Sciences. 2019 Mar;20(3):618.
9. Keane TJ, Badylak SF. Biomaterials for tissue engineering applications. Seminars in Pediatric Surgery. 2014 Mar;23(3):112–8.
10. Nie L, Suo J, Zou P, Feng S. Preparation and Properties of Biphasic Calcium Phosphate Scaffolds Multiply Coated with HA/PLLA Nanocomposites for Bone Tissue Engineering Applications. Journal of Nanomaterials. 2012 Mar;2012(1).
11. Li J, Guan S, Su J, Liang J, Cui L, Zhang K. The Development of Hyaluronic Acids Used for Skin Tissue Regeneration. Current Drug Delivery. 2021 Mar;18(7):836–46.
12. Venkatesan J, Vinodhini PA, Sudha PN, Kim SK. Chitin and Chitosan Composites for Bone Tissue Regeneration. 2014;59–81.
13. Lee JS, Baek SD, Venkatesan J, Bhatnagar I, Chang HK, Kim HT, et al. In vivo study of chitosan-natural nano hydroxyapatite scaffolds for bone tissue regeneration. International Journal of Biological Macromolecules. 2014 Mar; 67:360–6.
14. Zadpoor AA. Bone tissue regeneration: the role of scaffold geometry. Biomaterials Science. 2015;3(2):231–45.
15. Hollister SJ. Porous scaffold design for tissue engineering. Nature Materials. 2005 Mar;4(7):518–24.
16. Ambekar RS, Kandasubramanian B. Progress in the Advancement of Porous Biopolymer Scaffold: Tissue Engineering Application. Industrial & Engineering Chemistry Research. 2019 Mar;58(16):6163–94.
17. Zhang H, Zhou L, Zhang W. Control of Scaffold Degradation in Tissue Engineering: A Review. Tissue Engineering Part B: Reviews. 2014 Mar;20(5):492–502.
18. Koushik TM, Miller CM, Antunes E. Bone Tissue Engineering Scaffolds: Function of Multi-Material Hierarchically Structured Scaffolds. Advanced Healthcare Materials. 2023 Mar;12(9).
19. Liu Y, Shang Y, Wang Z, Gao H, Jin N, Zhang W, et al. From Microsphere Synthesis to Neural Tissue Regeneration: Unraveling the Potentials and Progress. Composites Part B: Engineering. 2025 Mar;112363.
20. Chen J, Du C, Tang B, Liu J, Xiao P, Wang X, et al. Application and progress of smart hydrogel microspheres for regulating oxidative stress in osteoarthritis. Chemical Engineering Journal. 2025 Mar;507:160620.
21. Wu X, Huo Y, Ci Z, Wang Y, Xu W, Bai B, et al. Biomimetic porous hydrogel scaffolds enabled vascular ingrowth and osteogenic differentiation for vascularized tissue-engineered bone regeneration. Applied Materials Today. 2022 Mar; 27:101478.
22. Kim M, Franco RA, Lee BT. Synthesis of functional gradient BCP/ZrO2 bone substitutes using ZrO2 and BCP nanopowders. Journal of the European Ceramic Society. 2011 Mar;31(9):1541–8.
23. Zeng W, Huang J, Hu X, Xiao W, Rong M, Yuan Z, et al. Ionically cross-linked chitosan microspheres for controlled release of bioactive nerve growth factor. International Journal of Pharmaceutics. 2011 Mar;421(2):283–90.
24. Pal K, Banthia AK, Majumdar DK. Preparation and characterization of polyvinyl alcohol-gelatin hydrogel membranes for biomedical applications. AAPS PharmSciTech. 2007 Mar;8(1):E142–6.
25. Kokubo T, Takadama H. How useful is SBF in predicting in vivo bone bioactivity? Biomaterials. 2006 Mar;27(15):2907–15.
26. Huang L, Zhou B, Wu H, Zheng L, Zhao J. Effect of apatite formation of biphasic calcium phosphate ceramic (BCP) on osteoblastogenesis using simulated body fluid (SBF) with or without bovine serum albumin (BSA). Materials Science and Engineering: C. 2017 Jan;70:955–61.
27. Macedo FA, Nunes EHM, Vasconcelos WL,

Santos RA, Sinisterra RD, Cortes ME. A biodegradable porous composite scaffold of PCL/BCP containing Ang-(1-7) for bone tissue engineering. Cerâmica. 2012 Mar;58(348):481–8.

28. Tajvar S, Hadjizadeh A, Samandari SS. Scaffold degradation in bone tissue engineering: An overview. International Biodeterioration & Biodegradation. 2023 Mar;180:105599.
29. Meesuk L, Suwanprateeb J, Thammarakcharoen F, Tantrawatpan C, Kheolamai P, Palang I, et al. Osteogenic differentiation and proliferation potentials of human bone marrow and umbilical cord-derived mesenchymal stem cells on the 3D-printed hydroxyapatite scaffolds. Scientific Reports. 2022 Mar;12(1):19509.
30. Cai H, Yao Y, Xu Y, Wang Q, Zou W, Liang J, et al. A Col I and BCP ceramic bi-layer scaffold implant promotes regeneration in osteochondral defects. RSC Advances. 2019;9(7):3740–8.
31. Yang Z, Xie L, Zhang B, Zhang G, Huo F, Zhou C, et al. Preparation of BMP-2/PDA-BCP Bioceramic Scaffold by DLP 3D Printing and its Ability for Inducing Continuous Bone Formation. Frontiers in Bioengineering and Biotechnology. 2022 Mar;10.
32. Li B, Ma Y, Fatima K, Zhou X, Chen S, He C. 3D Printed Scaffolds with Multistage Osteogenic Activity for Bone Defect Repair. Regenerative Biomaterials. 2025 Mar;
33. Wang J, Chen X, Yang X, Guo B, Li D, Zhu X, et al. Positive role of calcium phosphate ceramics regulated inflammation in the osteogenic differentiation of mesenchymal stem cells. Journal of Biomedical Materials Research Part A. 2020 Jun 24;108(6):1305–20.
34. Linh NTB, Jang DW, Lee BT. Collagen immobilization of multi-layered BCP-ZrO2 bone substitutes to enhance bone formation. Applied Surface Science. 2015 Mar;345:238–48.